Excitation and emission mechanisms of Er:GaN gain medium in 1.5 μm region

Z. Y. Sun, L. C. Tung, W. P. Zhao, J. Li, J. Y. Lin, and H. X. Jiang[a)]
Department of Electrical and Computer Engineering, Texas Tech University, Lubbock, Texas 79409, USA

(Received 1 June 2017; accepted 2 August 2017; published online 17 August 2017)

Er doped GaN (Er:GaN) is a very promising gain medium for realizing high energy lasers (HELs) operating in the relatively eyesafe 1.5 μm spectral region due to its high thermal conductivity, low thermal expansion coefficient, low temperature coefficient of the refractive index, and high atmospheric transmittance. We report the results of optical absorption and resonantly excited photoluminescence emission spectroscopy studies performed on Er:GaN freestanding quasi-bulk crystals grown by hydride vapor phase epitaxy. Fine features resulting from the transitions between Stark sublevels in the $^4I_{13/2}$ first excited state and $^4I_{15/2}$ ground state manifolds enabled the construction of energy level diagrams pertaining to the excitation and emission mechanisms of Er:GaN eyesafe HELs. Our results suggest that the most appropriate pump lines in Er:GaN are 1514 nm and 1539 nm, whereas the lasing emission lines are most likely to occur at 1569 nm and 1581 nm, conforming to the requirements of an extremely small quantum defect lasing system. In contrast to the more established HEL gain medium of Er:YAG, the well-known absorption (or pump) line near 1470 nm is absent in Er:GaN. Er:GaN HELs are expected to outperform those based on Er:YAG in terms of average power, power density, and beam quality. *Published by AIP Publishing.*
[http://dx.doi.org/10.1063/1.4985726]

The development of high energy and high power solid-state lasers has enabled extensive commercial, military, and scientific applications. The optical gain medium is the heart of a high energy laser system. Presently, dominant gain materials for solid-state high energy lasers (HELs) are synthetic garnets such as YAG doped with neodymium (Nd:YAG) emitting at 1.06 μm. On the other hand, laser sources emitting light around 1.5 μm are considered "eyesafe" because photons in this wavelength region are strongly absorbed by the cornea, thereby more effectively protecting the retina. It is known that the upper limit of eyesafe laser exposure at 1.5 μm is more than 4 orders of magnitude higher than that of the wavelengths below or close to 1 μm.[1,2] Furthermore, a 1.5 μm laser also has a high atmospheric transmittance.[3] Therefore, HELs operating around 1.5 μm are highly sought-after for use in defense, industrial processing, communications, medicine, spectroscopy, imaging, and various other applications where the laser is expected to travel long distances in free space. When doped in a host, the emission lines resulting from the intra-4f transitions from the first excited state manifold ($^4I_{13/2}$) to the ground state manifold ($^4I_{15/2}$) in Er^{3+} ions are near 1.5 μm.[4,5] HELs based on Er doped YAG (Er:YAG) have reached high performance levels.[6–11] However, with the relatively poor thermal properties of YAG with a thermal conductivity of $\kappa = 14$ W/m·K and the thermal expansion coefficient of $\alpha \approx 8 \times 10^{-6}\,^{\circ}C^{-1}$, the heat dissipation capability of YAG gain medium is relative poor, which limits the optical output energy, average power, and the beam quality.[12–15] Therefore, finding gain materials with improved thermal properties is highly desirable.

Of the wide bandgap III-nitride semiconductors which have demonstrated excellent performances in high power, high temperature electronics, and optoelectronics,[16–19] Er doped GaN (Er:GaN) is a promising gain medium for HEL. Compared to YAG, GaN has a much larger thermal conductivity ($\kappa = 253$ W/m·K for GaN versus 14 W/m·K for YAG),[20] lower thermal expansion coefficient ($\alpha \approx 3.53 \times 10^{-6}\,^{\circ}C^{-1}$ for GaN versus $8 \times 10^{-6}\,^{\circ}C^{-1}$ for YAG),[20] and lower temperature coefficient of the refractive index, dn/dT ($0.7 \times 10^{-5}\,^{\circ}C^{-1}$ for GaN versus $1.75 \times 10^{-5}\,^{\circ}C^{-1}$ for YAG).[21] Hence, HELs based on Er:GaN are expected to outperform those based on Er:YAG in terms of average power, power density, and beam quality. Due to the lack of thick crystals of Er:GaN, spectroscopic studies of Er:GaN so far have been mostly performed on epilayers of a few microns in thickness grown by metal organic chemical vapor deposition (MOCVD) or molecular beam epitaxy (MBE) with targeted applications of optoelectronic devices for optical communications in the infrared (IR) region and for emitters in the visible region.[22–34] However, to develop low quantum defect HEL operating in the eyesafe spectral region based on Er:GaN, it is desirable to investigate mechanisms for resonant excitation and emission in thick Er:GaN crystals so that most appropriate optical pumping schemes can be identified and developed. In this work, optical absorption and resonantly pumped photoluminescence (PL) emission spectra of freestanding Er:GaN quasi-bulk crystals have been measured, from which the energy level diagrams of the ground and first excited states in Er:GaN pertaining to achieving low quantum defect Er:GaN eyesafe lasers have been constructed.

Freestanding Er:GaN quasi-bulk crystals of 1 mm in thickness were obtained via growth by hydride vapor phase epitaxy (HVPE) in conjunction with a laser-lift-off process.[35] The Er doping concentration ranges from 5×10^{19} ions/cm^3 to 1×10^{20} ions/cm^3 as determined by secondary-ion mass spectrometry. The samples were then subjected to double side chemical-mechanical polishing. The final thickness of the sample used in this study was 600 μm. A broad light

a)hx.jiang@ttu.edu

source covering a wavelength range between 170 and 2100 nm coupled with a triple grating monochromator was used as a variable wavelength excitation source for the optical absorption measurements. The absorption setup provides an overall spectral resolution of 2 nm.

Figure 1(a) shows the room temperature optical absorption spectrum measured in the 1450–1650 nm region. The spectrum revealed two dominant absorption bands near 1514 nm and 1539 nm. Fitting the absorption spectrum using multiple Gaussian peaks also resolved a third peak near 1556 nm. A significant result is that there are nearly no features, and the absorption is extremely low below 1500 nm. This is in sharp contrast to the fact that Er^{3+} in most other host materials such YAG and silica glass exhibit a strong absorption line near 1470 nm, corresponding to a resonant transition between Stark sublevels, from the bottom of the $^4I_{15/2}$ ground state manifold to the top of the $^4I_{13/2}$ first excited state manifold. In fact, this transition line near 1470 nm is the most common pumping line employed for achieving Er:YAG lasers.[6–11]

Figure 1(b) shows the PL emission spectrum of the same Er:GaN sample measured at 250 K around 1.5 μm. The excitation source is a 980 nm laser diode, and the PL signal was collected using an InGaAs detector in conjunction with a spectrometer. It should be noted that in this excitation scheme, carriers were excited from the $^4I_{15/2}$ ground state to the $^4I_{11/2}$ second excited state manifolds of Er^{3+} ions and then relaxed to the $^4I_{13/2}$ first excited state manifolds through fast non-radiative transitions. The spontaneous emission lines around 1.54 μm are then given by the radiative intra-4*f* transitions from the first excited state to the ground state ($^4I_{13/2} \rightarrow {}^4I_{15/2}$) of Er^{3+} ions. Due to the involvement of this non-radiative relaxation process, 980 nm is therefore not a desired pump wavelength for achieving low quantum defect HELs. The spectral shape of the PL spectrum shown in Fig. 1(b) is rather similar to that of the absorption spectrum shown in Fig. 1(a) with a central peak near 1538 nm, but with additional fine features resulting from the transitions between Stark sublevels in the $^4I_{15/2}$ ground state and the $^4I_{13/2}$ first excited state manifolds, which were not resolved in the optical absorption spectrum. Consistent with the absorption spectrum, the PL spectrum is nearly featureless below 1500 nm, and the transition lines near 1470 nm widely observed in other host materials are absent in Er:GaN. In fact, the observed optical absorption peak positions are in good agreement with the peak positions of optical absorption cross section for the $^4I_{15/2}$ to $^4I_{13/2}$ transition observed in a waveguide fabricated from the Er:GaN epilayer grown by MOCVD.[32] Furthermore, the spectra shown in Fig. 1 are in excellent agreement with a previous crystal field analysis built on PL emission and excitation spectroscopy results of Er:GaN thin epilayers grown by MOCVD,[33] based on which the energy level diagram of Er^{3+} in the ground ($^4I_{15/2}$) and first excited ($^4I_{13/2}$) state manifolds in Er:GaN has been reconstructed, as shown in Fig. 1(c). The experimentally observed transition energies in Figs. 1(a) and 1(b) are indicated by the arrows in Fig. 1(c).

The energy level diagram shown in Fig. 1(c) reveals that there are multiple Stark sublevels in the $^4I_{13/2}$ first excited state manifolds, similar to the case in Er:YAG. Therefore, multiple optical absorption lines near 1514 nm are expected, despite the fact that they were not clearly resolved in Fig. 1(a) due to the spectral resolution limit of our optical absorption setup. To reveal further the desired excitation scheme, we measured the emission intensities at 1540 and 1558 nm for several excitation wavelengths, providing a crude PL

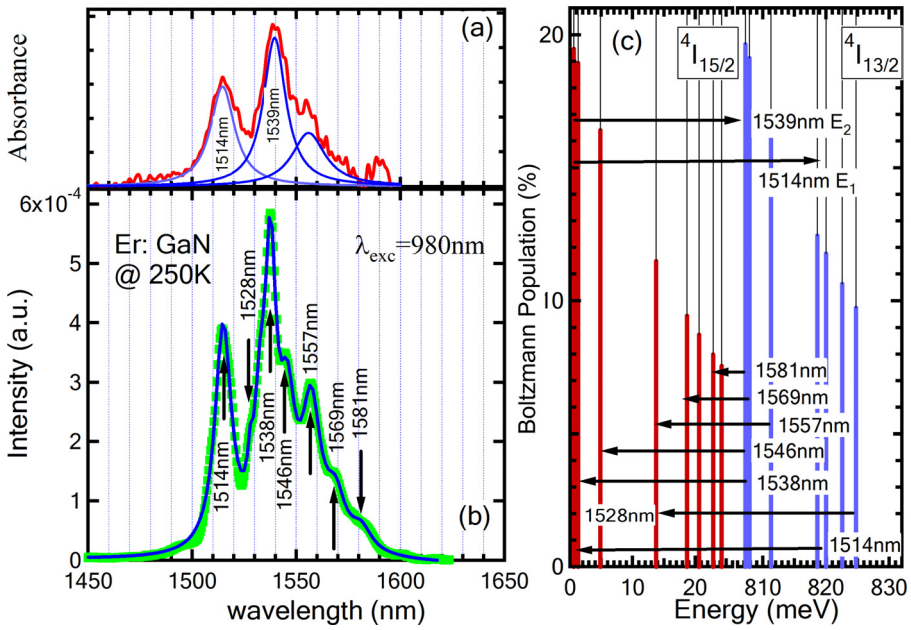

FIG. 1. (a) Optical absorption spectrum of an Er:GaN freestanding quasi-bulk crystal measured in the 1.5 μm spectral region with the 2 nm spectral resolution. (b) The PL emission spectrum of the same sample measured in the 1.5 μm spectral region with the excitation wavelength of $\lambda_{exc} = 980$ nm. (c) Energy level diagram of Er^{3+} in the ground ($^4I_{15/2}$) state and first excited ($^4I_{13/2}$) state manifolds in Er:GaN re-constructed from a previous crystal field analysis built on PL emission and excitation spectroscopy results of Er:GaN thin epilayers grown by MOCVD [reproduced with permission from Stachowicz *et al.*, Opt. Mater. **37**, 165 (2014). Copyright 2014 Elsevier],[33] and the observed lines in an Er:GaN freestanding quasi-bulk crystal shown in Fig. 1(a) for absorption and Fig. 1(b) for emission are indicated by arrows. The corresponding 300 K Boltzmann occupation factors for each energy level are indicated by the vertical bold solid lines.

excitation spectroscopy scheme. In obtaining the excitation spectra shown in Fig. 2, the variation in the excitation wavelength was obtained by changing the lasing wavelength of a laser diode (LD) around 1514 nm through the variation in the operating temperature of the LD. Figure 2 indeed revealed that the absorption maximum occurs at 1514 nm, but the acceptable pump wavelength window is broad covering roughly from 1510 nm to 1515 nm as expected from the energy level diagram shown Fig. 1(c) for the $^4I_{13/2}$ first excited state manifold. However, excitation spectroscopy studies covering a broad range and with a higher spectral resolution are desired in the future.

To gain insights into possible lasing wavelengths, we have measured the PL emission spectra excited by laser diodes with operating wavelengths tuned into the resonant excitation closely matching with the optical absorption maxima near 1514 and 1539 nm. The PL emission spectra under 1514 nm and 1540 nm excitation are shown in Figs. 3(a) and 3(b), respectively. Multiple emission lines resulting from the transitions between the Stark sublevels in the $^4I_{15/2}$ ground state and the $^4I_{13/2}$ first excited state manifolds have been resolved, with several lines that have been identified in the PL spectrum shown in Fig. 1(b) under 980 nm pump. Under resonant excitations, the most common emission lines beyond 1550 nm appear to be near 1557 nm, 1569 nm, and 1581 nm. It is interesting to note that the emission peaks become narrower as the resonant pump wavelength increases, and the PL spectrum under 1540 nm pump composed of sharpest lines. The fitted full width at half maximum (FWHM) of deconvolution Gaussian peaks is as narrow as 0.1 nm for the PL spectrum under 1540 nm excitation. This is understandable because the recombination under resonant excitation using the longest wavelength excites the least number of sublevels and involves the least steps of thermal relaxation processes, and so, the FWHM of emission lines approaches the true intrinsic characteristics of intra-4f shell transitions. The observation of narrow emission lines is indicative that the local site of Er ion in GaN bulk crystals is highly symmetric with no distortion.[30]

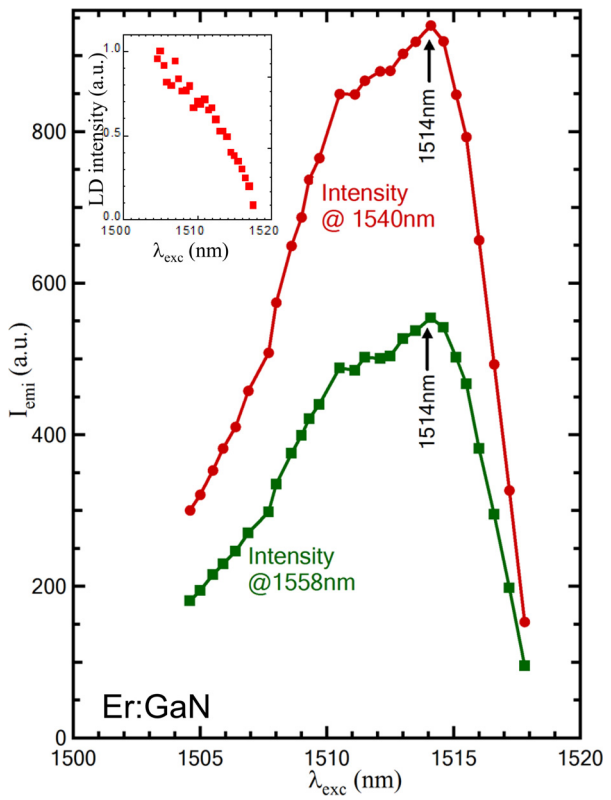

FIG. 2. Crude excitation spectra probed at 1540 nm and 1558 nm of an Er:GaN freestanding quasi-bulk crystal: Emission intensities probed at 1540 nm and 1558 nm as the excitation wavelength varied in a small range by changing the operating temperature of the laser diode (LD) used as an excitation source. The emission intensities have been normalized to the LD emission intensities at the corresponding excitation wavelengths. The inset shows the output intensity vs the excitation wavelength of the LD used.

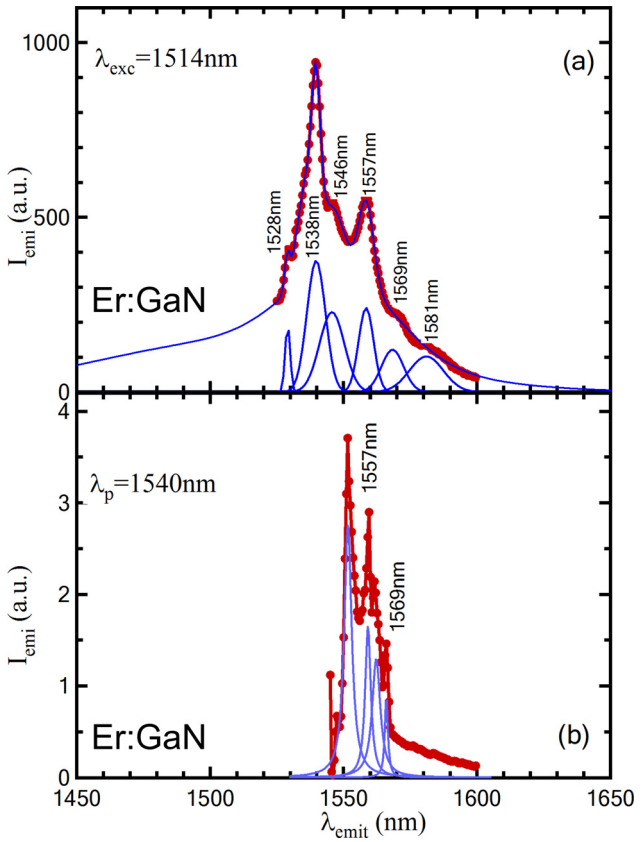

FIG. 3. Resonantly excited emission spectra measured near 1.5 μm of an Er:GaN freestanding quasi-bulk crystal with (a) $\lambda_{exc} = 1514$ nm and (b) $\lambda_{exc} = 1540$ nm.

One of the criteria for achieving lasing is to attain population inversion, which can be reached more easily if the upper laser level is easily populated, whereas the lower laser level is rapidly depopulated. With this in mind together with the observed optical absorption and emission lines, we have constructed in Fig. 4(a) the energy level diagram of the ground and first excited states to illustrate the most likely excitation and lasing scenarios in resonantly pumped eyesafe Er:GaN lasers. The results show that the most appropriate pump lines appear at 1514 nm and 1539 nm, whereas the lasing emission lines most likely to occur at 1569 nm and 1581 nm. For comparison, we also plotted the corresponding energy level diagram illustrating the well understood excitation and lasing schemes in resonantly pumped eyesafe Er:YAG lasers in Fig. 4(b). It can be seen that the differences between the pumping and lasing wavelengths in Er:GaN are smaller than those in Er:YAG for both the quasi-four-level and quasi-three-level lasing systems, implying that

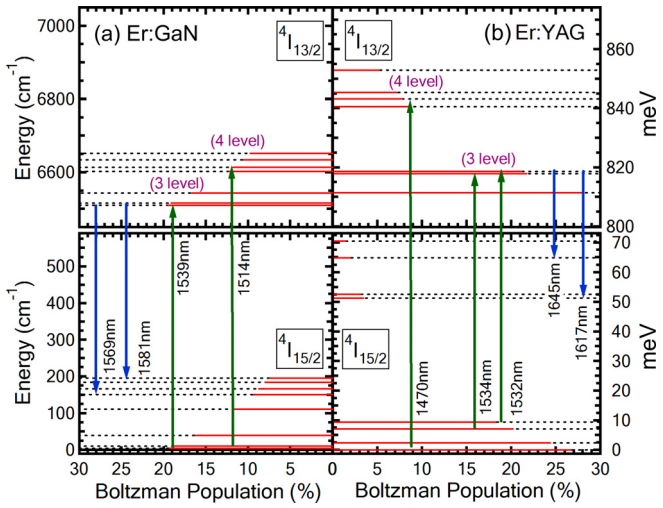

FIG. 4. (a) Energy level diagram constructed from the results of Figs. 1–3, providing the excitation and emission mechanisms of Er:GaN low quantum defect lasers operating near 1.5 μm. (b) The equivalent energy level diagram of Er:YAG lasers. 4 level and 3 level indicate a quasi-four-level and quasi-three-level system, respectively. The corresponding 300 K Boltzmann occupation factors for each energy level are indicated by the horizontal bold solid lines.

resonantly pumped eyesafe Er:GaN lasers potentially possess smaller quantum defects than those based on Er:YAG. Another potential advantage of Er:GaN is its expected lasing wavelength occurring below 1600 nm. It is known that the current state-of-the-art near IR tracking cameras used in eyesafe HEL systems are based on GaInAs epitaxial structures grown on lattice-matched InP, which have a bandgap of 0.75 eV and a cut-off wavelength of 1620 nm,[36] making these tracking cameras less sensitive and hence, more difficult to track the lasing wavelengths of Er:YAG than those of Er:GaN.

In summary, optical absorption and emission spectroscopy studies have been carried out for freestanding Er:GaN quasi-bulk crystals. It was shown that the well-known absorption line near 1470 nm in Er:YAG which is widely used as a pump line for Er:YAG eyesafe lasers is absent in Er:GaN. As a consequence, the energy level diagram and hence the common excitation and emission scheme of Er:YAG are not applicable to achieve Er:GaN eyesafe lasers. Optical absorption and resonantly excited PL emission spectra have provided an understanding of the energy level diagrams of the ground ($^4I_{15/2}$) state and first excited ($^4I_{13/2}$) state manifolds in Er:GaN. The results revealed that the most likely excitation and lasing scenario in resonantly pumped eyesafe Er:GaN lasers involves pump lines at 1514 nm and 1539 nm for a quasi-four-level and quasi-three-level system, respectively, and lasing emissions at 1569 nm and 1581 nm. In addition to higher thermal conductivity of Er:GaN over Er:YAG gain medium, Er:GaN eyesafe lasers appear to possess lower quantum defects than Er:YAG lasers.

The work was supported by High Energy Laser Joint Technology Office (Grant No. #W911NF-12-1-0330) monitored by Dr. Mike Gerhold of ARO. H. X. Jiang and J. Y. Lin would also like to acknowledge the support of Whitacre Endowed Chairs by the AT & T Foundation.

[1]Y. Kalisky and O. Kalisky, Opt. Eng. **49**, 091003 (2010).
[2]J. A. Zuclich, D. J. Lund, and B. E. Stuck, Health Phys. **92**, 15 (2007).
[3]J. Bailey, A. Simpson, and D. Crisp, Publ. Astron. Soc. Pac. **119**(852), 228 (2007).
[4]E. Desurvire, *Erbium-Doped Fibre Amplifiers: Principles and Applications* (John Wiley & Sons, 1994).
[5]M. J. Connelly, *Semiconductor Optical Amplifiers* (Springer, 2002).
[6]K. Spariosu, V. Leyva, R. A. Reeder, and M. J. Klotz, IEEE J. Quantum Electron. **42**, 182 (2006).
[7]J. O. White, IEEE J. Quantum Electron. **45**, 1213 (2009).
[8]N. Ter-Gabrielyan, V. Fromzel, X. Mu, H. Meissner, and M. Dubinskii, Opt. Lett. **38**, 2431 (2013).
[9]M. Němec, J. Šulc, L. Indra, M. Fibrich, and H. Jelínková, Laser Phys. **25**, 015803 (2015).
[10]T. Sanamyan, J. Opt. Soc. Am. B **33**, D1 (2016).
[11]D. J. Ottaway, L. Harris, and P. J. Veitch, Opt. Express **24**, 15341 (2016).
[12]G. Huber, C. Krankel, and K. Petermann, J. Opt. Soc. Am. **27**, B93 (2010).
[13]W. Koechner, *Solid-State Laser Engineering*, 5th ed. (Spring-Verlag, Berlin Heidelberg, 1999).
[14]J. Vetrovec, Proc. SPIE **4632**, 104 (2002).
[15]A. Giesen and J. Speiser, IEEE J. Sel. Top. Quantum Electron. **13**, 598 (2007).
[16]S. Nakamura, G. Fasol, and S. J. Pearton, *The Blue Laser Diode: The Complete Story* (Springer, New York, 2000).
[17]A. Bergh, G. Crawford, A. Duggal, and R. Haitz, Phys. Today **54**(12), 42 (2001).
[18]Y. Narukawa, M. Sano, M. Ichikawa, S. Minato, T. Sakamoto, T. Yamada, and T. Mukai, Jpn. J. Appl. Phys. Lett., Part 2 **46**, 963 (2007).
[19]J. Day, J. Li, D. Lie, C. Bradford, J. Lin, and H. Jiang, Appl. Phys. Lett. **99**, 031116 (2011).
[20]H. Shibata, Y. Waseda, H. Ohta, K. Kiyomi, K. Shimoyama, K. Fujito, H. Nagaoka, Y. Kagamitani, R. Simura, and T. Fukuda, Mater. Trans. **48**, 2782 (2007).
[21]R. Hui, Y. Wan, J. Li, S. Jin, J. Y. Lin, and H. X. Jiang, IEEE J. Quantum Electron. **41**, 100 (2005).
[22]P. N. Favennec, H. L'Haridon, M. Salvi, D. Moutonnet, and Y. Le Guillou, Electron. Lett. **25**, 718 (1989).
[23]J. Heikenfeld, M. Garter, D. S. Lee, R. Birkhahn, and A. J. Steckl, Appl. Phys. Lett. **75**, 1189 (1999).
[24]A. J. Steckl and J. M. Zavada, MRS Bull. **24**, 33 (1999).
[25]S. Kim, S. J. Rhee, X. Li, J. J. Coleman, and S. G. Bishop, Appl. Phys. Lett. **76**, 2403 (2000).
[26]C. Ugolini, N. Nepal, J. Y. Lin, H. X. Jiang, and J. M. Zavada, Appl. Phys. Lett. **89**, 151903 (2006).
[27]R. Dahal, C. Ugolini, J. Y. Lin, H. X. Jiang, and J. M. Zavada, Appl. Phys. Lett. **97**, 141109 (2010).
[28]V. Dierolf, "Combined excitation spectroscopy of RE ions in GaN," in *Rare-Earth Doped III-Nitrides for Optoelectronic and Spintronic Applications*, edited by K. O'Donnell and V. Dierolf (Canopus Academic Publishing Ltd and Springer SBM, 2010), Chapter 8.
[29]J. S. Filhol, R. Jones, M. J. Shaw, and P. R. Briddon, Appl. Phys. Lett. **84**, 2841 (2004).
[30]A. Braud, "RE excitation processes in GaN," in *Rare-Earth Doped III-Nitrides for Optoelectronic and Spintronic Applications*, edited by K. O'Donnell and V. Dierolf (Canopus Academic Publishing Ltd and Springer SBM, 2010), Chap. 8.
[31]D. K. George, M. D. Hawkins, M. McLaren, H. X. Jiang, J. Y. Lin, J. M. Zavada, and N. Q. Vinh, Appl. Phys. Lett. **107**, 171105 (2015).
[32]Q. Wang, R. Dahal, I.-W. Feng, J. Y. Lin, H. X. Jiang, and R. Hui, Appl. Phys. Lett. **99**, 121106 (2011).
[33]M. Stachowicz, A. Kozanecki, C. G. Ma, M. G. Brik, J. Y. Lin, H. X. Jiang, and J. M. Zavada, Opt. Mater. **37**, 165 (2014).
[34]I. W. Feng, X. K. Cao, J. Li, J. Y. Lin, H. X. Jiang, N. Sawaki, Y. Honda, T. Tanikawa, and J. M. Zavada, Appl. Phys. Lett. **98**, 081102 (2011).
[35]Z. Y. Sun, J. Li, W. P. Zhao, J. Y. Lin, and H. X. Jiang, Appl. Phys. Lett. **109**, 052101 (2016).
[36]A. Rogalski, Infrared Phys. Technol. **43**, 187 (2002).